SOIL RESISTANCE PREDICTIONS FROM PILE DYNAMICS

By Frank Rausche,[1] Fred Moses,[2] A.M. ASCE and George G. Goble,[3] M. ASCE

This paper was originally published in the September, 1972, issue of the Journal of the Soil Mechanics and Foundations Division, ASCE. It is reprinted here with the permission of ASCE

ABSTRACT: An automated prediction scheme is presented which utilizes both force and acceleration records measured at the pile top during driving to compute the soil resistance forces acting along the pile. The distribution of these forces is determined, and the dynamic and static resistance forces are distinguished such that a prediction of a theoretical static load versus penetration curve is possible. As a theoretical basis stress wave theory is used, derived from the general solution of the linear one-dimensional wave equation. As a means of calculating the dynamic pile response, a lumped mass pile model is devised and solved by the Newmark β-method. Wave theory is also employed to develop a simple method for computing static bearing capacity from acceleration and force measurements. Twenty-four pile tests are reported, 14 of them with special instrumentation, i.e., strain gages along the pile below grade. The piles tested were of 12-in. (30-cm) diameter steel pipe with lengths ranging from 33 ft. to 83 ft. (10 m to 25 m).

INTRODUCTION

Observations made during impact driving are widely used to predict the static bearing capacity of piles. The results often do not agree with static load tests due to a lack of knowledge of hammer energy, cushion characteristics, set per blow and other factors. Recent developments in electronics have made it possible to make accurate records of force and acceleration at the pile top during impact driving. Such records,

[1] Asst. Prof. of Engrg., Case Western Reserve Univ., Cleveland, Ohio.
[2] Assoc. Prof. of Engrg., Case Western Reserve Univ., Cleveland, Ohio.
[3] Prof. of Civ. Engrg., Case Western Reserve Univ., Cleveland, Ohio.

which last only a matter of milliseconds, will be used herein to predict soil resistance effects on the pile. Previous work done on this project by a group at Case Western Reserve University reported the use of force and acceleration records in a simplified model to predict static bearing capacity (4, 5, 6, 11). These results were based on impact records which were taken after a setup period so that strength changes due to soil remolding or porewater pressure dissipation were included.

The present work extends the application of the force and acceleration records to the calculation of the distribution of soil resistance along the pile. It also shows how the records are used to predict the magnitude of dynamic resistance that the soil applies to the pile, an important factor in choosing efficient hammer characteristics. A method for obtaining a more accurate simplified prediction of total static bearing capacity is also presented. It should be emphasized that the aforementioned predictions are all made from measurements at the pile top only. The work is correlated by presentation of results for 24 pile tests which include construction static load tests as well as specially instrumented load test piles.

The application of these results can have considerable impact on foundation costs. Static load tests are very costly and time consuming. In Ohio a single test on a service pile using tension reaction piles (also service piles) typically costs $3,000 to $5,000. This static test provides much useful information about the particular pile which was tested. However, due to variability of soil properties the information may be of less value for other piles in the structure. This is reflected in the large factors of safety commonly used for piles. The proposed dynamic measurements methods can be applied to a substantial number of service piles at less than the cost of a single static load test.

The dynamic analysis herein differs from the general dynamics problem in which either the boundary force or acceleration record is given as input and the other record calculated as output. In the present dynamic analysis, both force and acceleration are shown and thus one of the two records can be viewed as redundant information. The second record is, therefore, used in the present analysis to give information on pile resistance effects; e.g., in the absence of soil resistance, the acceleration at the pile top completely determines the force at the top from Newton's and Hooke's laws. The presence of resistance along the pile and at the pile tip affects the force at the top in a precise and predictable manner and makes it possible to compute the magnitude and location of resistance forces along the pile. A simple soil resistance model is used, which consists of an elastoplastic shear resistance and a linear viscous damper. The dynamic analysis will be reviewed herein to present the basic ideas behind the work. The detailed mathematical expressions are given in Refs. 3 and 9.

Details of the instrumentation have been presented previously (6). Force records were obtained from either strain gage transducers or gages attached directly to the pile. The piezoelectric accelerometers used during the project have been quite satisfactory. Instrumentation has been developed to the point where the necessary dynamic measurements can be made with an interruption of less than 30 min in the driving operation.

DYNAMIC STRESS WAVE ANALYSIS

This section describes the solution of the one-dimensional wave problem in an elastic rod to determine the soil resistance forces acting on a pile during impact. The important fact is that measurements are available of both force and acceleration at the pile top during impact driving. In the usual dynamics problem where the external boundary conditions are known, either force or acceleration is used as input and the other quantity is then calculated, in a dynamic analysis, as the output. In the following analysis both force and acceleration records are available and used to determine the soil resistance characteristics as the output including static and dynamic values. The static resistance distribution and the dynamic forces are determined.

A pile under impact can be analyzed for stresses and displacements by use of a lumped mass analysis. In such an analysis the pile is divided into elements whose elastic and inertial properties are represented by springs and lumped masses, respectively. Spring-mass models used in such an analysis have been considered by Smith (12) and other investigators (2, 7, 10). In the proposed method for predicting soil resistance distribution, it is necessary to perform several pile analyses. Herein Smith's analysis is extended by use of a predictor-corrector numerical integration scheme (the so called Newmark β-method). It is both more accurate and more efficient than currently used techniques for dynamic analysis of piles (3).

For obtaining qualitative results and an insight into the propagation of hammer applied forces, the analysis of a continuous elastic pile is useful. Investigations of this kind go back to St. Venant, and analyses by Donnell (1) and Timoshenko (13) are summarized and extended in Ref. 3. Results important to a pile dynamic analysis are briefly stated in the following without proof. A stress wave is due to a difference in stress between neighboring cross sections causing particle motions such that a balance exists between inertia forces and stresses. In a uniform unsupported elastic pile, the stress gradient will travel unchanged through the rod so that the particle velocity is known for a point along the rod if it was known at some time at another location. The speed of wave propagation, c, depends only on the material properties of the rod, i.e., Young's Modulus E and mass density ?.

When the stress wave arrives at an end, the stress gradient will be changed; e.g., at a free end the particles will be subjected to much higher accelerations because no further material is strained. The dynamic balance can be maintained only if another stress wave travels away from the end. At a free end such a reflection wave will change the sign of the stresses. At a fixed end, where the stresses build up and no acceleration of particles is possible, the particle motion in the reflection wave will be in the opposite direction. If a force, such as a skin friction, is applied at some intermediate point along the rod, a tension and a compression stress will be induced on opposite sides of the point, causing two stress waves to travel in opposite directions away from the force. In a uniform rod these two waves will have the same stress magnitudes with opposite signs.

For the present analysis, records of force and acceleration, continuous over time, are available. The acceleration record is used as a boundary condition at the pile top and the soil resistance properties are adjusted until the computed output force at the top matches the measured top force. The approach used herein is to first compute the

force on top of a free pile with the velocity record, computed by numerical integration from the acceleration, prescribed as the top boundary condition. The difference between the computed free pile force and the measured pile top force is the force due to the soil action. Thus, a resistance force versus time relation is found.

To understand the meaning of these force difference curves, the soil effects have to be examined. An analogous free pile has measured input velocity at the top and zero external forces along its length and bottom end. The actual pile in the ground has the same velocity at the top and the real force acting along its length and at the bottom end. Thus, the top force difference between the free pile and the actually measured solution is a force acting at the top of a fixed pile due to the action of the resistance forces. This difference will be called the measured delta curve.

Fig. 1 shows such a delta curve for an actual pile record. Curve a is the measured velocity record (multiplied by a proportionality constant EA/c, where A is the pile cross-sectional area) at the top determined directly from the acceleration record by numerical integration. Curve b shows the measured force. Curve c shows the force at the top associated with an assumed free pile with no resistance along its length and subjected to curve a as a velocity input at the top. Curve d is the delta curve which is the difference between measured force b and the force computed from the velocity record, c. Note that curves b and c are similar until some point after the impact reaches its maximum. The later deviation between the curves shows the soil resistance being reflected upwards and felt at the top of the pile.

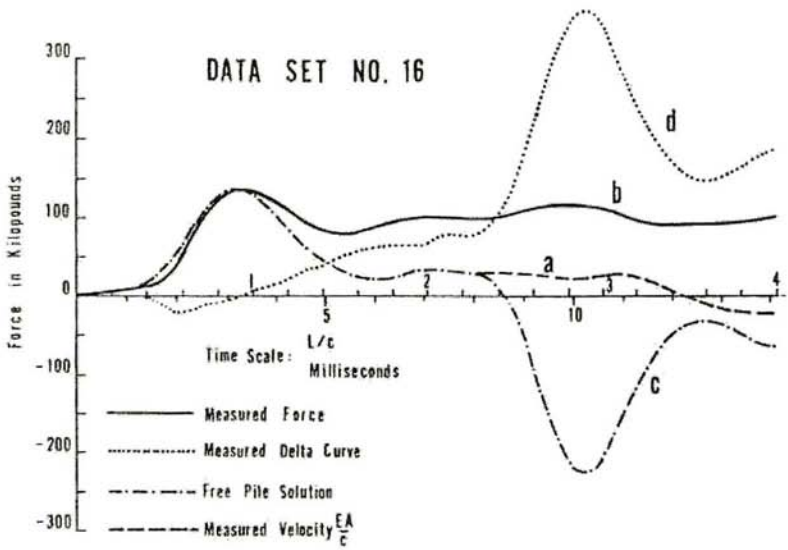

FIG.1. Measured Force and Velocity, Proportional, Derived Free Pile Solution and Measure Delta Curve

In order to interpret the measured delta curve correctly, it is necessary to adopt a soil model which links pile displacements and velocities to soil resistance forces. The shear strength versus deformation behavior can be represented as a first approximation by a straight line until at a certain deflection-called quake in the pile dynamics literature-the ultimate shear resistance is reached. Thereafter the soil strength usually increases at a rate smaller than in the beginning of the curve and can be neglected in dealing with relatively small dynamic displacements. For increasing displacements greater than the quake the stiffness then is assumed to be zero. The value of the quake has been found not to be critical for pile driving analysis (2). In analyzing actual pile records, it is always assumed that a final set was obtained under the individual hammer blow considered. This condition places an upper bound on the quake values, as the quake must be smaller than the maximum displacement occurring at all points along the pile. It was found that the displacement reached at the time of maximum velocity can be a good estimate (3) for the quake. Using this value reduces the number of unknowns in the soil model, as the value of the ultimate shear strength now describes the shear versus displacement behavior completely.

Using the model of a linear damper, dynamic resistance forces will be assumed to be proportional to pile velocities. As in the case of a shear resistance force, a damper will induce waves which travel in both directions along the pile. The stress waves due to dampers continually change magnitude to reflect the rapid changes in velocity during impact driving.

The action of a resistance force at some particular point along the pile or at the pile tip can be represented by a resistance delta curve. This is defined as the force induced on a fixed pile top while the bottom end is free and only the resistance force under investigation acts along the pile. It includes both the effect of the resistance wave moving upwards and the resistance wave moving downwards and subsequently reflected from the pile tip. In the case of a shear force, the resistance delta curve reaches a level value because of the assumed elastoplastic sail resistance model. Consequently, the shear resistance is seen at the top as a constant value until the effect of stress reversal is felt, making it possible to compute both its magnitude and location along the pile. The magnitude of resistance is determined from the force felt at the top and the location of resistance from the time after impact required for the wave to reach the top. For the case of a shear resistance force acting at the pile tip, the resistance delta curve is shown in Fig. 2. It can be observed that at time $2L/c$ (the time required for the stress wave to travel the length of the pile and return) after the maximum velocity due to the reflections, the value of the resistance delta curve becomes twice the ultimate shear resistance force (in this case 2 x 44.0 kips = 2 x 196 kN). Fig. 2 shows a resistance delta curve for a damper at the toe. Note that the shear resistance effect maintains a constant value while the damper resistance effect drops off quickly due to the decrease in the velocity. This important difference permits the two types of soil resistance forces to be distinguished.

The measured delta curve considered previously represents the superposition of resistance delta curves for all soil forces acting at various locations along the pile. Because each soil resistance force takes a longer time to reach the top at increasingly lower depths along the pile, each level of resistance can be isolated separately. Thus,

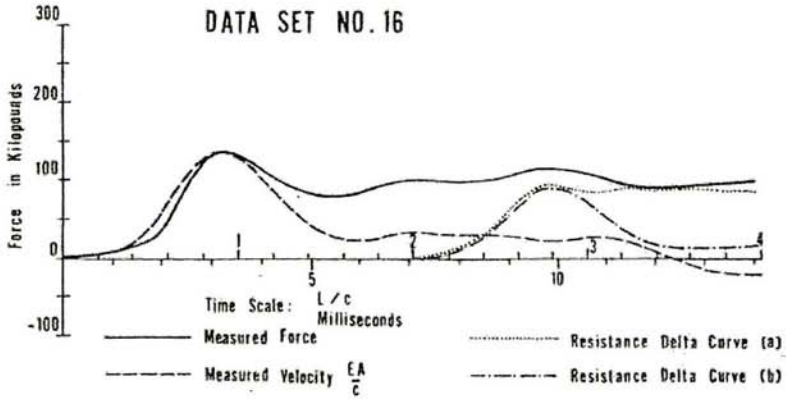

FIG. 2. Measured Force and Velocity (Proportional); *(a)* Resistance Delta curve for Shear at Bottom (44 kips = 196 kN); *(b)* Resistance Delta Curve for Damper at bottom ($d_i = 0.2\ EA/c$)

from the early time portion of the measured delta curve, predictions about the locations and magnitudes of resistance forces can be made. The separation of soil damping from shear resistance effects is made from the latter part of the record where the shear forces remain on and the damping forces drop off as described previously.

This idea of the delta curves has been used to develop an automated routine for predicting both shear and dynamic resistance forces acting on the pile skin and pile tip during the first period after hammer impact. The considerations of stress waves due to resistance forces indicated that from the early portion of the measured delta curve conclusions could be drawn on the location of resistance forces and that from the variation of the delta curve a criterion could be derived for separating dynamic from shear resistance forces. As it was not possible, with the soil model used, to obtain criteria which would clearly indicate locations of dynamic forces, several damping force distributions along the pile are tried and then a final selection made based on the best possible overall match between predicted and measured force plots.

In a first trial, the dynamic forces are concentrated at the bottom end of the pile. An assumed magnitude of the dynamic forces can be found from the simplified models to be analyzed subsequently. A resistance delta curve due to this damper is computed and subtracted from the measured delta giving a reduced function which reflects only the effects of shear resistance forces. Because resistance forces located near the top show their full effect at an earlier time than the forces below, it is possible to compute in succession the magnitude of resistance forces along the pile.

The procedure is repeated iteratively to eliminate errors that result from neglecting interactive effects of resistance force. For finding errors, the predicted resistance values are placed at corresponding elements of a lumped mass pile model and a dynamic analysis is performed which produces a new predicted top force. The difference between the measured force and this prediction is a new delta curve that

indicates the errors in the predicted resistance force distribution and provides a basis for determining corrections. The process is repeated until the match cannot be further improved. Resulting matches between measured and predicted force records will be illustrated.

Other analyses are also used, with the dynamic forces uniformly distribution along the pile or apportioned between skin and toe, with little change in predicted capacity but differences in top force matches. Subsequently, a final prediction is computed by minimizing a least square integral of the final delta curves. This can be accomplished by linear combination of the three individual sets of results and leads to a damping and shear resistance distribution with the best possible match.

The preceding method of dynamically analyzing a pile using measured in-put quantities has limitations which should be mentioned. First, and most important, it was found from acceleration and force records taken at the pile bottom (3) that the soil model only approximates the soil behavior. Cohesive soils showed a less satisfactory agreement than cohesionless soils. Second, the method requires that the hammer impact produces a stress wave with a short rise time. If, as an extreme example, the loading were of a static nature, then no distinction between locations of resistance forces were possible. Finally, it is not possible to predict the distribution of damping and static resistance forces independently. For this reason the method was designed to optimize the match between measured and computed pile top force. This approach might fail where large damping is encountered because of the limitations of the soil model. To introduce another soil model could improve the method. Work is currently being done in this area.

SIMPLIFIED METHODS

These methods also use the force and acceleration records and have been incorporated by the Ohio Department of Highways for use in special purpose field computers for construction control during driving (4, 5). The first method, denoted as Phase 1, is based on a rigid body pile model and, in order to eliminate damping effects, on equilibrium at the instant when the pile velocity is zero. In this case the static resistance R_0 is given by

$$R_0 = F(t_0) - Ma(t_0) \tag{1}$$

in which t_0 = the time of zero velocity at the pile top; M = pile mass; $F(t_0)$ the top force at time t_0; and $a(t_0)$ = the top acceleration at time t_0.

Because of the oscillations of the force and acceleration records in the neighborhood of t_0, due primarily to pile-hammer interaction, the results of Phase I have exhibited considerable scatter. To improve the predictions, a Phase 11 method was proposed (6) which eliminated the oscillation effect of the acceleration by taking average values. This gives the static bearing capacity as

$$R_0 = F(t_0) - \frac{M}{t_1 - t_2} \int_{t_2}^{t_1} a(t)dt \tag{2}$$

Usually t_1, is taken as the time of maximum force and t_2 is set equal to t_0 the time of zero velocity.

The Phase II method has been improved upon recently by use of the dynamic traveling wave analysis and leads to the following result denoted as Phase IIa (3):

$$R_0 = \frac{F(t_1) + F\left(t_1 + \frac{2L}{c}\right)}{2} - \frac{M}{2L} \int_{t_1}^{t_1 + (2L/c)} a(t)\, dt \qquad (3)$$

$$c$$

In other words, the best averaging scheme from a theoretical point of view is that which takes averages over a time equal to the period of oscillation, $2L/c$. To eliminate as much as possible the dynamic viscous effects, t_1 is set equal to t_0, in Eq. 3. A modification of this choice of t_1 must be employed in cases where the velocity reaches no zero value within the analyzed record (Piles with low capacity reach zero velocity often only a long time after impact). Such modifications are reported in Ref. 3. The comparison of the simplified Phases I, II and IIa with the more exact traveling wave solution is presented and analyzed in the following.

CORRELATION PROCEDURE

Experimental data were obtained from both specially instrumented and construction load test piles. Complete sets of data were available for analysis from 24 tests. A description of the piles is given in Table 1.

Several results can be predicted from a single data set when applying the methods reviewed previously. These predictions are summarized as follows: (1) Static bearing capacity; (2) shear resistance distribution along the pile; and (3) pile top force during static loading versus pile penetration.

The latter item is predicted by using the shear resistance forces along the pile in a static load-displacement analysis and the assumed elastoplastic soil model. Such an analysis produces a pile top force versus displacement relation which can be compared with the same curve from the actual field load test.

Load versus deflection curves obtained in a static load test often show increasing strength values with pile top deflections much larger than those which are reached under a hammer blow. Thus, the prediction of static bearing capacity from dynamic measurements must be related to displacements of the pile actually experienced under the blow. A question arises, therefore, as to the value with which to compare the predicted bearing capacity.

Using data set No. 3 as an example, this question will now be examined. Wave analysis was applied to this data set and both damping and shear resistance forces were predicted. The predicted shear resistance distribution was then used for a static analysis. The load versus penetration (LP) curve resulting from this analysis and the corresponding curve measured in the field static load test are both plotted in Fig. 3(b). Both LP curves show similar behavior up to a point where the predicted load curve reaches its ultimate capacity. The measured LP curve, however, shows further strength increase without an indication that an ultimate bearing capacity is reached.

TABLE 1.-Description of Test Piles

Data set number (1)	Pile name (2)	Date			Length, *L*, (Below Accelerometer) in feet (6)	Area, A, in square inches (7)	Hammer (8)
		Driven (3)	Statically Tested (4)	Dynamicall y tested (5)			
1	C-1	12-28/66	12-30-66	1-3-67	58	5.81	D-12[a]
2	531-70	4-12-67	5-12-67	4-13-67	70	5.81	D-12
3	531-76	4-13-67	4-17-67	4-18-67	82	5.81	D-12
4	531-83	4-18-67	4-18-67	5-18-67	82	5.81	D-12
5	F-30	6-21-67	6-21-67	6-21-67	32.5	9.82	LB[b]
6	F-30A	6-21-6-67	6-28-67	6-28-67	32.5	9.82	LB
7	F-50	6-28-67	6-28-67	6-28-67	50.5	9.82	LB
8	F-50A	6-28-67	7-5-67	7-6-67	50.5	9.82	LB
9	F60	7-7-67	7-7-67	7-7-67	59.5	9.82	LB
10	F-60A	7-7-67	7-20-67	7-20-67	59.5	9.82	LB
11	Cincinnati	12-22-67	1-4-68	1-4-68	69	6.66	D-12
12	272 Toledo	4-10-68	4-17-68	5-18-68	54	6.66	LB
13	To-50	9-6-68	9-6-68	9-6-68	49	9.82	D-12
14	To-50A	9-6-68	9-9-68	9-10-68	49	9.82	D-12
15	To-60	9-11-68	9-11-68	9-11-68	59	9.82	D-12
16	To-60A	9-11-68	9-18-68	9-18-68	59	9.82	D-12
17	Logan	11-25-68	11-5-68	11-5-68	57	6.66	D-12
18	W-56	6-11-69	6-18-69	6-18-69	55	6.66	D-12
19	W-76	6-19-69	6-24-69	6-24-69	76	6.66	D-12
20	Chillicothe	6-18-69	6-25-69	9-25-69	40.5	6.66	D-12
21	Ri-50	1-6-70	1-6-70	1-6-70	49	9.31	D-12
22	Ri-50	1-6-70	1-6-70	1-6-70	49	9.31	D-12
23	Ri-60	1-9-170	1-9-70	1-9-70	61.5	9.31	D-12

All piles were of 12-in. diam pipe
1 ft = 0.305m.; 1 in. = 2.54 cm

[a]D-12 = Delmag
[b]LB = Linkbelt 440.

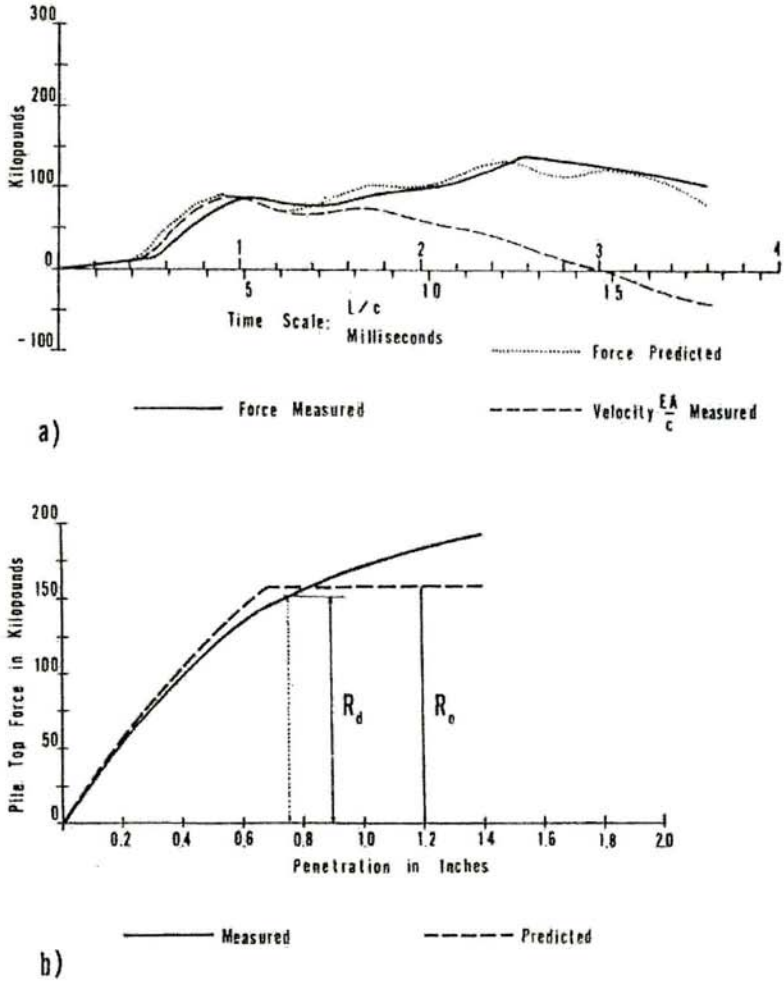

FIG. 3. Data Set No. 3: *(a)* Comparison between Measured and Predicted Pile Top Force and Measured Pile Top Velocity; *(b)* Comparison between Measured and Predicted Static Load Versus Penetration Curve

In a static test, a load is applied on top of the pile which compresses both the pile and the soil. The elastic pile deformations were relatively large for the piles encountered in this study. (The pile of the data set No. 3, for example, compresses 0.52 in. = 1.32 cm under a uniform load of 100 kips = 445 kN). Because of pile elastic deformations, the pile tip moves less than the pile top and during a static load

test the pile tip will usually be the last point along the pile to reach the quake penetration. If the assumed static elastoplastic soil resistance law were valid, then the ultimate capacity would be reached at that pile top penetration occurring when the tip reaches the quake displacement. This is the case only for the assumed soil model; but in reality, the soil resistance forces frequently increase even after the quake penetration is exceeded, although at a smaller rate. Then a higher dynamic penetration will produce a higher shear resistance. Because the pile penetrations during driving are usually small, the assumed elastoplastic relationship still establishes a good approximation for the dynamic case. However, the static load test will not reach, at various points along the pile, the same penetration values simultaneously as the dynamic load and comparison between the dynamic prediction and static load test cannot be exact. In order to find a reasonable comparison between the static load test result and the dynamic prediction, the following correlation scheme is, therefore, proposed: From the dynamic analysis compute the maximum deflection of the pile top under the hammer blow and obtain the corresponding load value from the LP curve of the field static load test. Call load R_d the bearing capacity at maximum dynamic deflection. The predicted capacity from dynamic measurements R_0 will then be compared with R_d . For most cases, the static load penetration curve has leveled off at the maximum dynamic deflection, and differences with other definitions of bearing capacity (yield, ultimate) are small.

RESULTS

In this section, the results of applying wave analysis and simplified predictions to all data sets listed in Table 1 are reviewed and compared with results of the static load test. Exceptions were data sets Nos. 1, 2, 4, and 12, in which the wave analysis could not be applied because the rise time of force and velocity was longer than 2L/c, so that reflection waves returned from the pile bottom before the maximum velocity was reached at the pile top. The reason for such records is probably an early combustion in the hammer which cushioned the blow excessively.

Simplified Methods - The results from three simplified methods introduced previously are listed in Cols. 5, 6 and 7 of Table 2. Usually more than one blow had been analyzed. The average value was listed in Table 2.

Comparing the simplified predictions with the pile capacity at maximum dynamic deflection R_d in Col. 3, it can be seen that Phase IIa usually gave the better agreement. Some of the individual piles will be subsequently analyzed in connection with wave analysis results.

Wave Analysis - As an example, consider pile 531-76 (data set No. 3) having a record with the usual impact properties. Fig. 3(a) shows a plot of the top forces both predicted by wave analysis and measured. Also, the velocity measured at the pile top (used as input for the analysis) is plotted after being multiplied by *EA/c*. Agreement between predicted and measured pile top force is good throughout the time interval considered. Fig. 3(b) represents the LP curves both measured and predicted. The force at the point where the maximum dynamic deflection, shown by the dotted line, intersects the measured LP curve is R_d. Thus, correlation between R_d and R_0 the ultimate bearing capacity predicted, is good (see also Table 2). Fig. 4 shows both a

TABLE 2. Summary of Results for Prediction Static Bearing Capacity using Simplified Methods and Wave Analysis

		Load Test Results[a]		Predictions[b]					
Data set number	Pile name	At maximum dynamic deflection, R_d	At ultimate R_u	Phase I, R_0	Phase II, R_0	Phase IIa, R_0	Wave[d] analysis R_0	Wave[e] analysis, R_0	Total[e] damping forces, max D
(1)	(2)	(3)	(4)	(5)	(6)	(7)	(8)	(9)	(10)
1	C-1	180	192	174[1]	138[1]	176[3]	c	c	c
2	531-70	122	190	201[3]	197[3]	141[3]	c	c	c
3	531-76	151	198	170[4]	157[4]	115[4]	159[1]	159	15
4	531-83	110	200	211[3]	187[3]	143[3]	c	c	c
5	F-30	97	103	125[5]	113[5]	110[5]	88	88	39
6	F-30A	107	114	162[4]	152[4]	164[5]	136	136	24
7	F-50	172	224	281[3]	197[3]	177[3]	167	167	41
8	F-50A	200	238	294[4]	258[4]	205[4]	230	230	52
9	F-60	176	204	288[4]	251[4]	207[4]	200	200	25
10	F-60A	174	242	255[3]	226[3]	188[3]	198	198	52
11	Cincinnati	137	190	250[3]	185[3]	138[3]			
12	272	183	221	315[7]	275[7]	267[7]	c	c	c
13	To-50	60	69	69[3]	63[3]	77[5]	62	62	57
14	To-50A	93	94	121[8]	129[8]	105[8]	119	119	88
15	To-60	32	43	89[4]	81[4]	77[4]	55	55	69
16	To-60A	75	86	141[3]	137[3]	113[3]	119	119	106
17	Logan	165	220	275[4]	223[4]	180[4]			
18	W-56	90	92	207[4]	227[4]	161[4]			
19	W-76	125	160	276[5]	264[5]	167[3]			
20	Chilicothe	152	207	316[3]	200[3]	180[3]			
21	Ri-50	40	46	g	g	64[3]	45	45	88
22	Ri-50A	64	64	g	g	120[3]	85	85	105
23	Ri-60	176	f	264[3]	251[3]	140[3]	189	189	92
24	Ri-60A	174	f	1792	1842	1623	194	194	48

[a]All results in kips (1 kip = 4.45 kN)
[b]Superscripts on predictions indicate the number of blows analyzed and averaged.
[c]Not analyzed by wave method because of weak impact.
[d]Analysis results from more than one blow.
[e]Analysis results from one blow corresponding to Figs. 3 through 6.
[f]Load test incomplete.
[g]No zero velocity was reached within record analyzed.

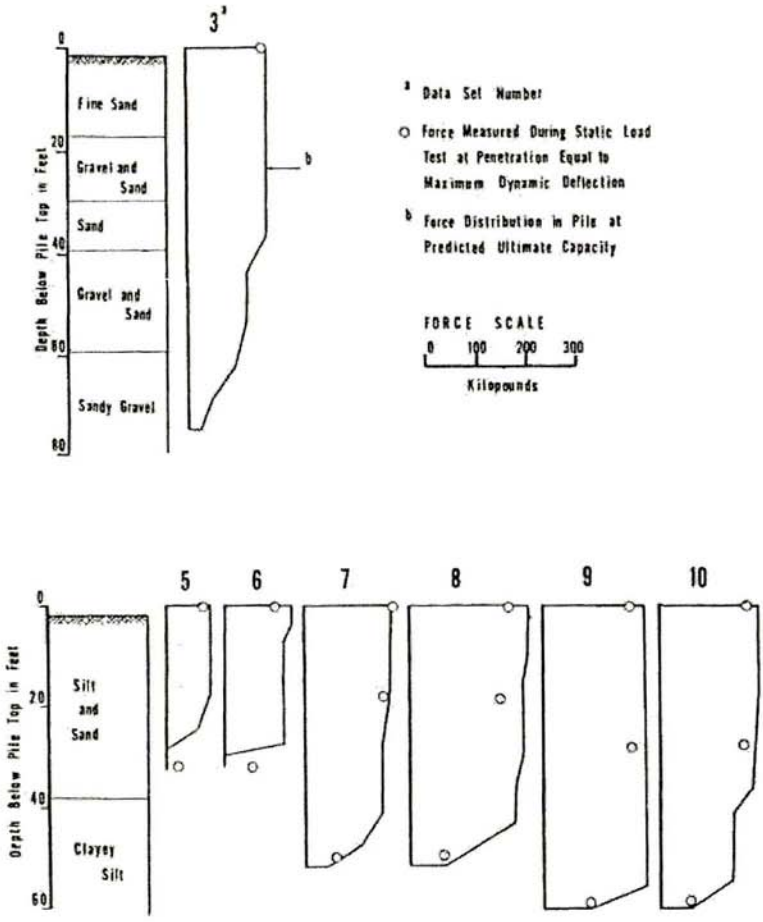

FIG. 4. Soil Description and Predicted Force Distribution I Pile at Predicted Ultimate Capacity

soil description and the predicted resistance force distribution in the pile (at maximum dynamic deflection).

The predicted shear resistance forces are acting at the lower pile half and are distributed rather uniformly. Because this pile was an actual construction pile, no force measurements were obtained from locations below grade. However, the blow count (number of blows per unit pile penetration) gradually increased with depth, thus providing some correlation with the prediction of resistance distribution.

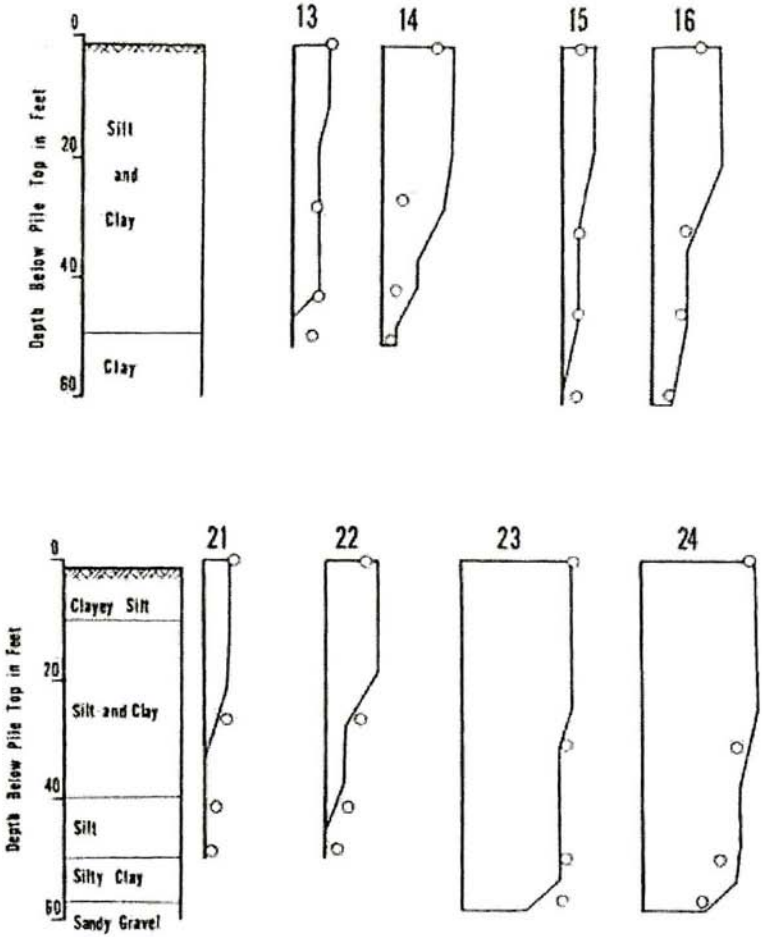

FIG. 4 Continued

Dynamic resistance forces predicted were small and concentrated at the pile tip. The magnitude of the sum of the maxima of all dynamic forces is listed in Table 2, Col. 10.

Fig. 5(a) shows the match of measured and predicted pile top force for data set No. 10. The pile was a special test pile with additional strain gages at the pile tip and close to the pile center. The data were obtained after a setup period of 1 week after driving. The predicted bearing capacity R0 (listed in Table 2, Col. 9), of 198 kips

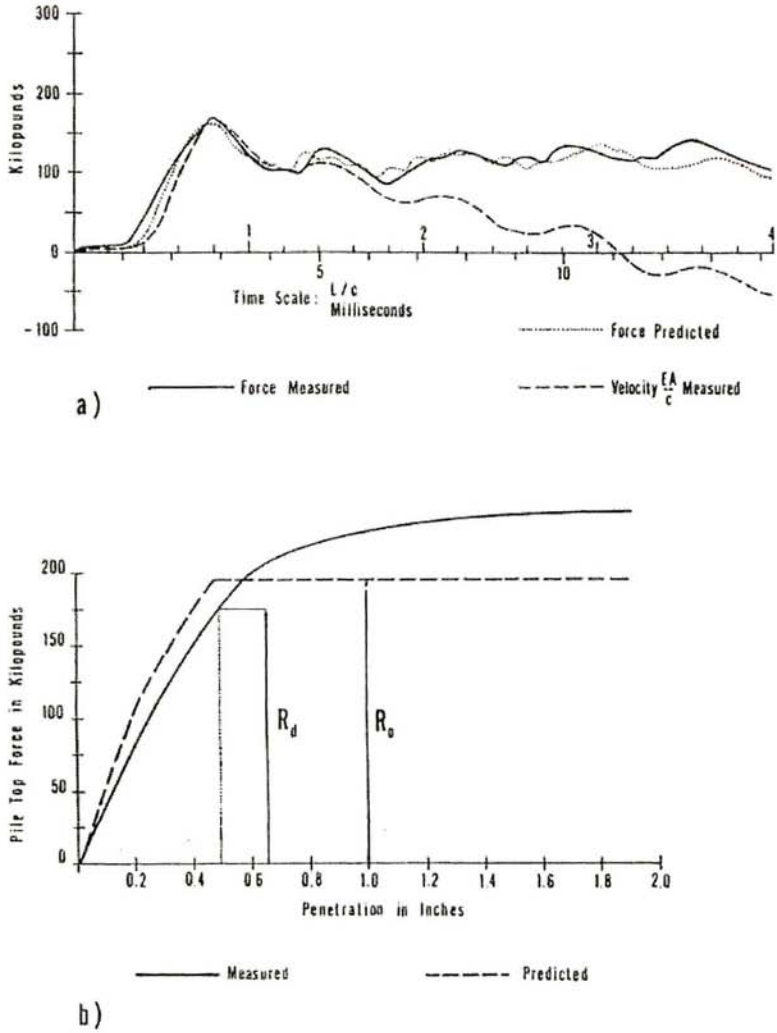

FIG. 5. Data Set No. 10: (a) Comparison between Measured and Predicted Pile Top Force and Measured Pile Top Velocity; (b) Comparison between Measured and Predicted Static Load versus Penetration Curve

(880kN) is somewhat higher than the static load test result R_d = 174 kips (775 kN) (Table 2, Col. 3). However, R_d was found at a deflection where the LP is still steeply increasing so that small errors in the preceding proposed correlation technique do

affect the agreement. Better agreement with measured results is usually obtained by analyzing several blows, as indicated in Table 2. Both measurements and predictions (see Fig. 4) indicate that most of the static resistance results from point bearing. The maximum dynamic resistance (all damping was predicted to act concentrated at the pile top) was approximately 25% of the total static bearing capacity (see Table 2).

The results for another special instrumented test pile (data set No. 16) are summarized in Figs. 5 and 6. The soil was highly cohesive, which explains why the maximum damping force predictions are approximately equal to the sum of the shear resistance forces (Table 2). Although the prediction of static bearing capacity was too high (119 kips versus 75, i.e., 530 kN versus 333), a clear indication of the importance of skin friction forces on the pile was found.

Data sets Nos. 5 through 10 were obtained at the same pile but for different lengths and both before and after a setup period. Data sets Nos. 5 and 6 were obtained when the pile was only 33.5 ft (10.2 m) long. During the static load test strain measurements were taken at both the top and the pile toe. The match between the predicted and measured pile top forces was poor at time $2L/c$ after maximum velocity and later. Agreement is good between R_0 from wave analysis and R_d for data set No. 5 and fair for data set No. 6. A deficiency of the predictions can be found in the distribution of shear resistance forces (Fig. 4). Apparently, the wave method failed to predict the proper pile tip resistance force. However, a shift of the predictions over one analysis element (10 elements were always used for the computations presented) is equivalent to a time shift of only 0.2 msec (the time necessary for the wave to travel 1/10 of the pile length). The accuracy of both the measurements and the method seems not to be sufficient to distinguish forces acting over such small distances.

Data set No. 7 was obtained after extending the aforementioned 33.5-ft (10.2-m) long pile by an additional section of 18 ft (5.5 in). Strain records were taken at three locations along the pile during the static load tests. The shear resistance distribution shows more pile tip resistance in the prediction than in the measurements. However, the fact that the pile had basically point bearing properties is brought out in both measurement and prediction. The results from analyzing data set No. 9 were very similar to those for set No. 10, which have already been considered.

Piles To-50 and To-60 were two special test piles of 50-ft and 60-ft (15.3-m and 18.3-m) length equipped with strain gages for force measurements below grade. Data set No. 13 was obtained immediately after driving pile To-50 and data set No. 14 after a setup period of 3 days. The soil was a silty clay. A low ultimate capacity of 69 kips (307 kN) was found in the load test immediately after driving. The predictions are good as shown in Fig. 4 and in Table 2.

Data set No. 14 yielded a bearing capacity which was too high. From force measurements along the pile taken during the load test it was found that relatively large resistance forces were acting along the skin of the pile. Apparently, these skin forces were predicted for locations lower than found in the static load test probably the uncertainty about damping distribution, mentioned above, lead to this result. The magnitude of the pile toe force, however, was predicted correctly.

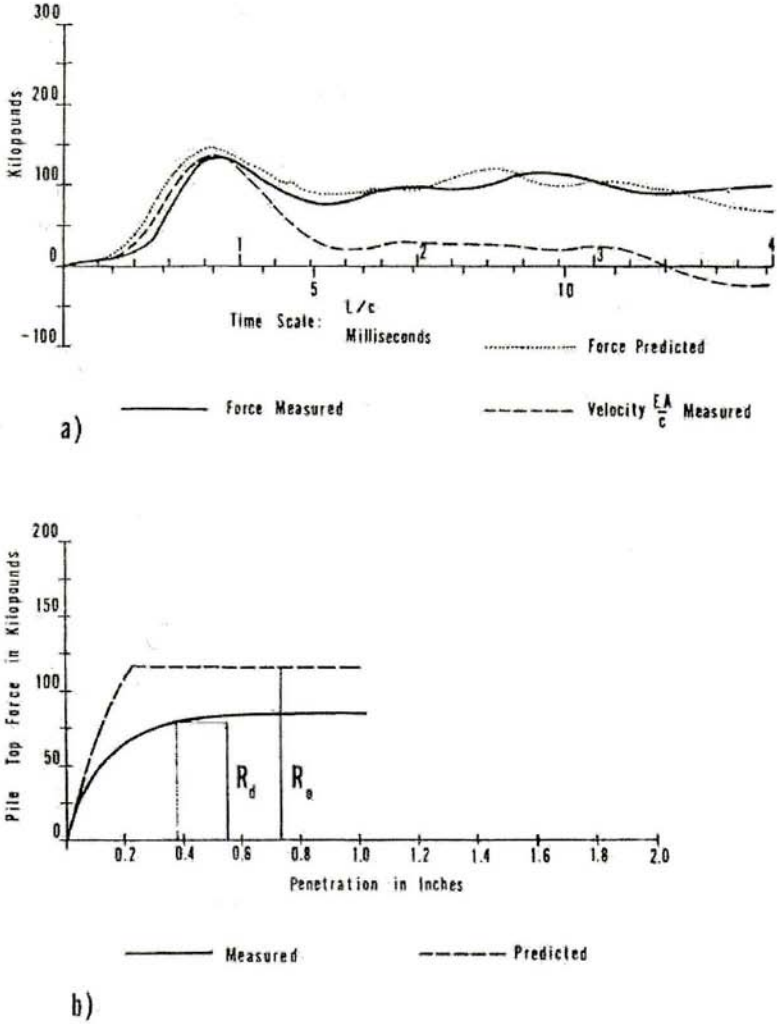

FIG. 6. Data Set No. 16: *(a)* Comparison between Measured and Predicted Pile Top Force and Measured Pile Top Velocity; *(b)* Comparison between Measured and Predicted Static Load Versus Penetration Curve

Data sets Nos. 15 and 16 were obtained from the second special test pile at the same site as the pile just reviewed. The pile was longer; however, its ultimate bearing capacity was smaller than for the shorter pile. Very similar observations as in Nos. 13

and 14 can be made on the results of both data sets. (Table 2 and Fig. 4). Data set No. 16 was previously considered.

Finally, results from another special test pile are presented. The pile was driven and tested in two steps. First the pile, Ri-50, was driven to a depth of 48 ft (14.6 m). This pile was embedded in silty and clayey soil (Fig. 4). Later the pile was driven until a stiff soil layer was reached and driving became very hard (Ri-60). The two data sets (Nos. 21 and 22) for the shorter pile gave results similar to the test piles To-50 and To-60 (data sets Nos. 13 through 16). The difference was that the waiting period did not influence the soil properties as much as in the case of the To-piles. Again, as in other cases of piles in cohesive soils, relatively high dynamic and skin resistance forces were observed. It should be mentioned that measurements and analysis correctly reflected the strength gain of shear forces along the pile skin during the waiting period. This can be seen by comparing the force distributions along the pile for data sets Nos. 21 and 22 in Fig. 4.

Other results from construction piles are also listed in Table 2. In these cases no measurements had been taken along the pile, so that resistance distributions cannot be compared. In general, it was found that piles in granular, materials (Nos. 11, 17 and 20) showed a point bearing distribution while the, two W piles (Nos. 18 and 19) were of the skin friction type. These two piles were driven in soils with plasticity indexes in the neighborhood of 15.

It should be mentioned that the prediction of ultimate capacity (Table 2, Col. 6) was poorest for pile W-56, probably because of the cohesiveness of the soil. The poorest correlation between dynamic predictions and static tests on a percentage basis occurred for piles having a very small capacity. Actually, such piles are not typical of practice and a percentage comparison is perhaps inappropriate.

STATISTICAL INVESTIGATION ON BEARING CAPACITY PREDICTIONS

A brief statistical investigation of the Phase IIa and wave analysis results was performed. Twenty sets of predictions are available including all data sets which were analyzed by the automated prediction routine. The variety of soil conditions represented is a fairly representative statistical sample. The computations are done as suggested by Olson and Flaate (8) for the treatment of results from the energy formulas. Accordingly, the, measured capacity, R_d, is thought of as being a function of the predicted capacity, R_0. A best fit straight line

$$R_d = m R_0 + b \tag{4}$$

is then determined for the prediction scheme by the least square method, The results are shown in Figs. 7(a) and 7(b) for the Phase IIa and the wave analysis, respectively. As a measure of the variability in the predictions the variances,

σ_m^2 *and* σ_b^2 *of* m and b, are also calculated. For illustrations, the lines

$$R_d = (m \pm s_m) R_0 + (b \pm s_b) \tag{5}$$

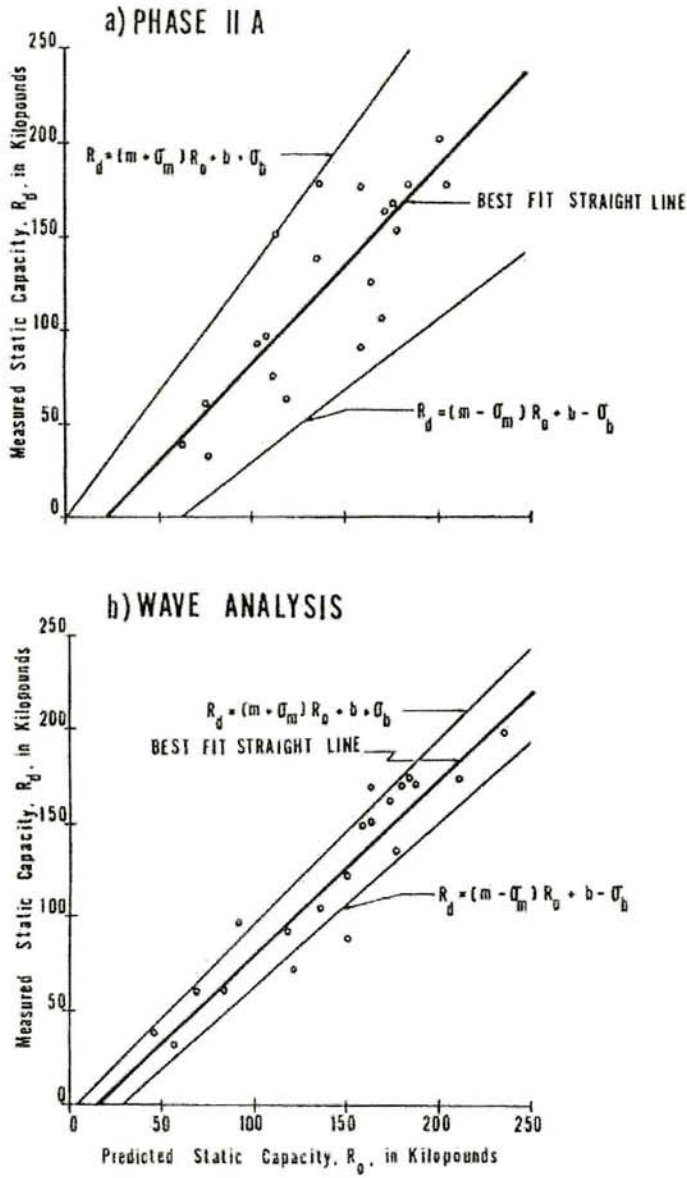

FIG. 7. Results from Statistical Analysis for 20 Predictions

are plotted together with the best fit lines. Table 3 lists all parameters calculated together with the correlation coefficient for the two methods under investigation. Also, the results of statistical investigations on data from 93 piles in sandy soils (8) are given for comparison.

The best predictions resulted from the wave analysis method. This is as expected because the wave analysis includes both the dynamic and static portions of the resistance. But even the simplified method, Phase IIa, yields a better correlation coefficient than any of the energy formulas. It should be observed that from the 20 sets of data under investigation, 9 were taken on piles in cohesive soils, while the data in Ref. 8 were all from piles in sandy soils. Because larger differences occurred for cohesive soils, the present methods would yield even better accuracy if applied to only noncohesive soils.

TABLE 3.-Statistical Parameters for Simplified Method, Phase IIa, Wave Analysis and Energy Formulas

Method (1)	Slope $m \pm s_m$ (2)	Intercept, in kips, $b \pm s_b$ (3)	Correlation coefficient, ? (4)	Number of piles analyzed (5)
Phase IIa	0.99 ± 0.15	-19 ± 22	0.83	20
Wave Analysis	0.95 ± 0.07	-11 ± 10	0.94	20
Engineering News	0.33	+74	0.29	93
Gow	0.32	+74	0.36	93
Hiley	0.92	+14	0.72	93
Pacific Coast	1.04	+14	0.76	93
Janbu	0.87	+20	0.76	93
Danish	0.77	-4	0.81	93
Gates	1.81	-96	.81	93
1 kip = 4.45 kN				

SUMMARY

The previous analysis uses dynamic force and acceleration measurements, a traveling wave theory, and a lumped mass analysis, in conjunction with a soil model regarding the relation between soil forces and pile motion. The results show the location and magnitude of dynamic and static soil resistances forces acting on the pile during a hammer blow. The static soil resistance forces correspond to those forces acting on the pile during static loading. Another facet of the work is the development of a simple prediction scheme for static bearing capacity based on wave theory.

The field measurements of force and acceleration proved to be accurate enough for commonly encountered construction piles. The records were sufficient to predict the magnitude and distribution of the soil resistance forces as long as the soil model was adequate. Distinction of soil force types regarding their velocity or displacement dependency was very successful for piles in sandy soils. For cohesive soils an improved soil dynamics model may be useful.

The present method bypasses a major shortcoming of pile dynamic analyses found in the literature, namely the uncertainty of hammer input and soil parameters. In fact, the prediction scheme can be used to give information on soil behavior. This is in contrast to the usual procedures of first obtaining the soil properties by laboratory testing and then performing the pile analysis. Also information from the analysis may be obtained which would indicate characteristics of hammer types that would be most efficient for driving in particular soils. This is being studied further.

The predictions of static bearing capacity show a better correlation than those obtained from existing methods (8, 11). Another important result of the studies presented herein was the improvement of an existing simplified prediction scheme for static bearing capacity. As a further step to a realistic dynamic pile testing procedure, the Phase IIa prediction scheme was incorporated in a special purpose computer which is currently being tested on actual construction piles. Additional tests on piles with materials such as timber and concrete, piles of greater length and of variable cross section will be performed to further check the proposed methods.

It is expected that the proposed method will reduce foundation costs. First, static load tests will be less frequently necessary. Probably more important will be the use of these analyses and predictions to reduce the rather large margins between indicated bearing and capacity required by design. The economic use of multiple dynamic test piles, perhaps in conjunction with a single static test pile, will further add to the reliability of test results. Certainly the correlation between dynamic prediction and static measurement on the large number of piles tested cannot be ignored.

ACKNOWLEDGMENTS

The work reported herein was sponsored by the Ohio Department of Highways and the Bureau of Public Roads. The writers would like to express their appreciation to C. R. Hanes, R. M. Dowalter and R. A. Grover, all of the Ohio Department of Highways for their advice and assistance. The opinions, findings and conclusions expressed in this publication are those of the writers and not necessarily those of the State or the Bureau of Public Roads.

APPENDIX I.-REFERENCES

1. Donnell, L. B., "Longitudinal Wave Transmission and Impact," *Journal of Applied Mechanics*. Transactions, ASME, APM-52-14, 1930.
2. Forehand, P. W., and Reese, J. L., "Predictions of Pile Capacity by the Wave Equation," *Journal of the Soil Mechanics and Foundations Division*, ASCE, Vol. 90, No. SM2, Proc. Paper 3820, March, 1964, pp. 1-25.
3. Goble, G. G., Rausche, F., and Moses, F., "Dynamic Studies on the Bearing Capacity of Piles - Phase III," Final *Report to the Ohio Department of Highways*, Case Western Reserve Univ., Cleveland, Ohio, Aug., 1970.
4. Goble, G. G., and Rausche, F., "Pile Load Test by Impact Driving," *Highway), Research Record No. 333, Pile Foundations*, Highway Research Board, Washington, D.C., 1970.

5. Goble, G. G., Scanlan, R, H., and Tomko, J. J., "Dynamic Studies on the Bearing Capacity of Piles," *Highway Research Record No. 167, Bridges and Structures*, Highway Research Board, Washington, D.C., 1967.
6. Goble, G. G., et al., "Dynamic Studies on the Bearing Capacity of Piles-Phase II," *Final Report to the Ohio Department of Highways*, Case Western Reserve Univ., Cleveland, Ohio, July 1, 1968.
7. Lowery, L. L., et al., "Pile Driving Analysis-State-of-the-Art," *Research Report 33-13 (Final)*, Texas Transportation Institute, Texas A & M Univ., Jan. 1969
8. Olson, R. E., and Flaate, K. S., "Pile Driving Formulas for Friction Piles in Sand," *Journal of the Soil Mechanics and Foundations Division*, ASCE, Vol. 93, No. SM6. Proc. Paper 5604, Nov., 1967, pp. 279-296.
9. Rausche, F., "Soil Response from Dynamic Analysis and Measurements on Piles," thesis presented to the Case Western Reserve University, at Cleveland, Ohio, in 1970, in partial fulfillment of the requirements for the degree of Doctor of Philosophy.
10. Samson, C. H., Hirsch, T. L., and Lowery, L. L., "Computer Study of Dynamic Behavior of Piling," *Journal of the Structural Division*. ASCE, Vol. 89, No. ST4, Proc. Paper 3608, Aug., 1963, pp. 413-450.
11. Scanlan, R. H., and Tomko, J. J., "Dynamic Prediction of Pile Static Bearing Capacity," *Journal of the Soil Mechanics and Foundations Division*, ASCE, Vol. 95, No. SM2, Proc. Paper 6468, Mar., 1969, pp. 583-604.
12. Smith, E. A. L., "Pile Driving Analysis by the Wave Equation," *Journal of the Soil Mechanics and Foundations Division*, ASCE, Vol. 86, No. SM4, Proc. Paper 2574, Aug., 1960, pp. 35-61.
13. Timoshenko, S., and Goodier, J. M., McGraw-Hill Book Co., 2nd ed., 1951, p.438.

APPENDIX II.-NOTATION

The following symbols are used in this paper:

A = pile cross-sectional area;
$a(t)$ = pile top acceleration;
b = intercept of best fit straight line (Eq. 4);
c = wave speed in pile;
E = Young's modulus of pile material;
$F(t)$ = pile top force;
L = pile length;
M = pile mass;
m = slope of best fit straight line;
$max\ D$ = sum of maxima of all damping forces;
R_d = measured static pile capacity at maximum dynamic deflection;
R_0 = predicted static pile capacity;
R_u = measured ultimate static pile capacity;
? = correlation coefficient;
t = time variable;

t_0 = time of zero velocity;
t_1, t_2 = fixed time values;
? = mass density of pile material;
s_b = standard deviation of intercept (Eq. 5); and
s_m = standard deviation of slope (Eq. 5).